Supplementary Material for
Luminance-aware Color Transform for Multiple Exposure Correction

Jong-Hyeon Baek[1†] DaeHyun Kim[1†] Su-Min Choi[2] Hyo-jun Lee[1] Hanul Kim[3] Yeong Jun Koh[1*]
[1]Chungnam National University [2]42dot Inc.
[3]Seoul National University of Science and Technology
whdgusdl97@gmail.com, seven776484@gmail, sumin.choi@42dot.ai,
gywns6287@gmail.com, hukim@seoultech.ac.kr, yjkoh@cnu.ac.kr

S-1. Ablation study on SICE [2]

Tables S-1∼S-6 show ablation studieson SICE for the proposed components: luminance comparison module (LCM); post-processing module (PPM); the number of transformation functions (n); loss functions.

Table S-1 validates the effectiveness of the proposed LCM on the SICE dataset. The proposed network shows the best performance on SICE than the proposed network without LPM or without order learning (OL). Table S-2 shows the exposure correction performance according to the number of inverted residual (IR) blocks in PPM. We experimentally choose five IR blocks, which provide the best performance. Tables S-3 and S-4 demonstrate that our loss strategy is effective for multiple exposure correction. Table S-5 lists the performance according to the number of transformation functions (n). In general, multiple transformation functions per channel ($n > 3$) surpass single transformation function per channel ($n = 3$). Thus, we use multiple transformation functions and experimentally pick $n = 36$. Finally, Table S-6 shows the performance by varying loss weights λ_f and λ_p. We select the weights $\lambda_f = 0.5$ and $\lambda_p = 0.05$, resulting in the best PSNR and SSIM scores on average.

Methods	Under		Over		Average	
	PSNR	SSIM	PSNR	SSIM	PSNR	SSIM
w/o LCM	21.65	0.748	21.63	0.767	21.64	0.760
w/o $\mathcal{L}_1$	21.66	0.755	21.75	0.769	21.73	0.765
w/o OL	21.74	0.755	**21.91**	0.770	21.79	0.767
Ours	**22.34**	**0.773**	21.76	**0.771**	**22.02**	**0.772**

Table S-1. Ablation study for LCM. The best results are boldfaced.

S-2. Visualization of luminance features

Figure S-1 visualizes the embedding space of luminance features, extracted from the proposed luminance comparison module, using t-SNE method. Luminance features are extracted from all test images in the ME [1] dataset. For visibility, we manually divide the extracted features into five clusters according to the average luminance values of the test images. Those clusters are depicted in different colors as in Figure S-1. We observe that the luminance features are

# of IR	Under		Over		Average	
	PSNR	SSIM	PSNR	SSIM	PSNR	SSIM
0	21.28	0.748	21.26	0.769	21.27	0.762
1	21.51	0.757	21.58	0.769	21.53	0.767
2	23.21	0.856	23.38	0.867	21.62	0.765
3	22.04	0.761	21.69	0.754	21.89	0.771
7	21.75	0.751	**21.82**	0.771	21.80	0.765
5 (Ours)	**22.34**	**0.773**	21.76	**0.771**	**22.02**	**0.772**

Table S-2. Ablation study for the number of IR blocks in PPM. The best results are boldfaced.

Methods	Under		Over		Average	
	PSNR	SSIM	PSNR	SSIM	PSNR	SSIM
$\mathcal{L}_c$	21.31	0.747	21.51	0.759	21.38	0.750
$\mathcal{L}_c + \mathcal{L}_p$	21.64	0.744	21.44	0.754	21.52	0.751
$\mathcal{L}_c+\mathcal{L}_p+\mathcal{L}_f$	**22.34**	**0.773**	**21.76**	**0.771**	**22.02**	**0.772**

Table S-3. Ablation study for loss functions. The best results are boldfaced.

Methods	Under		Over		Average	
	PSNR	SSIM	PSNR	SSIM	PSNR	SSIM
w/o $\mathcal{L}_e$ for $\mathbf{Y}_L$	22.21	0.761	**21.84**	**0.775**	21.92	0.769
All (Ours)	**22.34**	**0.773**	21.76	0.771	**22.02**	**0.772**

Table S-4. Ablation study for the additional exposure correction loss for $\mathbf{Y}_L$. The best results are boldfaced.

n_t	Under		Over		Average	
	PSNR	SSIM	PSNR	SSIM	PSNR	SSIM
3	21.67	0.753	21.53	0.767	21.60	0.763
9	21.65	0.755	21.64	0.771	21.65	0.766
15	21.88	0.758	**21.94**	**0.775**	21.92	0.768
36 (Ours)	**22.34**	0.773	21.76	0.771	**22.02**	**0.772**

Table S-5. Ablation study for the number of intensity transformation functions. The best results are boldfaced.

Loss weight		Under		Over		Average	
λ_f	λ_p	PSNR	SSIM	PSNR	SSIM	PSNR	SSIM
0.5	0.1	22.04	0.757	21.79	0.778	21.89	0.770
1.0	0.05	21.78	0.759	21.74	0.770	21.72	0.769
1.0	0.1	21.99	0.762	**21.80**	**0.778**	21.93	0.769
0.5	**0.05**	**22.34**	**0.773**	21.76	0.771	**22.02**	**0.772**

Table S-6. Ablation study for various loss weights. The best results are boldfaced.

faithfully aligned, which indicates that they have the luminance information to support multiple exposure correction.

Figure S-1. t-SNE visualization of the luminance features of test images in the ME dataset.

S-3. Qualitative Results

Figures S-2 and S-3 qualitatively compares the proposed method with the state-of-the-arts on ME and SICE, respectively. In these examples, the proposed method corrects both overexposure and underexposure images to have more similar color-tones to their ground-truths than DBRN-ENC [3] and FECNet [4]. Figures S-4 and S-5 show exposure correction results with LCM, without LCM, and without order learning. Without LCM or order learning, the proposed network fails to produce reliable exposure correction results. In contrast, the proposed network with LCM yields visually pleasing images that have similar color-tones to the ground-truths. These examples validate the effectiveness of the proposed LCM with order learning.

References

[1] Mahmoud Afifi, Konstantinos G Derpanis, Bjorn Ommer, and Michael S Brown. Learning multi-scale photo exposure correction. In *CVPR*, pages 9157–9167, 2021. 1

[2] Jianrui Cai, Shuhang Gu, and Lei Zhang. Learning a deep single image contrast enhancer from multi-exposure images. volume 27, pages 2049–2062, 2018. 1

[3] Jie Huang, Yajing Liu, Xueyang Fu, Man Zhou, Yang Wang, Feng Zhao, and Zhiwei Xiong. Exposure normalization and compensation for multiple-exposure correction. In *CVPR*, pages 6043–6052, 2022. 2, 3, 4

[4] Jie Huang, Yajing Liu, Feng Zhao, Keyu Yan, Jinghao Zhang, Yukun Huang, Man Zhou, and Zhiwei Xiong. Deep fourier-based exposure correction network with spatial-frequency interaction. In *ECCV*, pages 163–180. Springer, 2022. 2, 3, 4

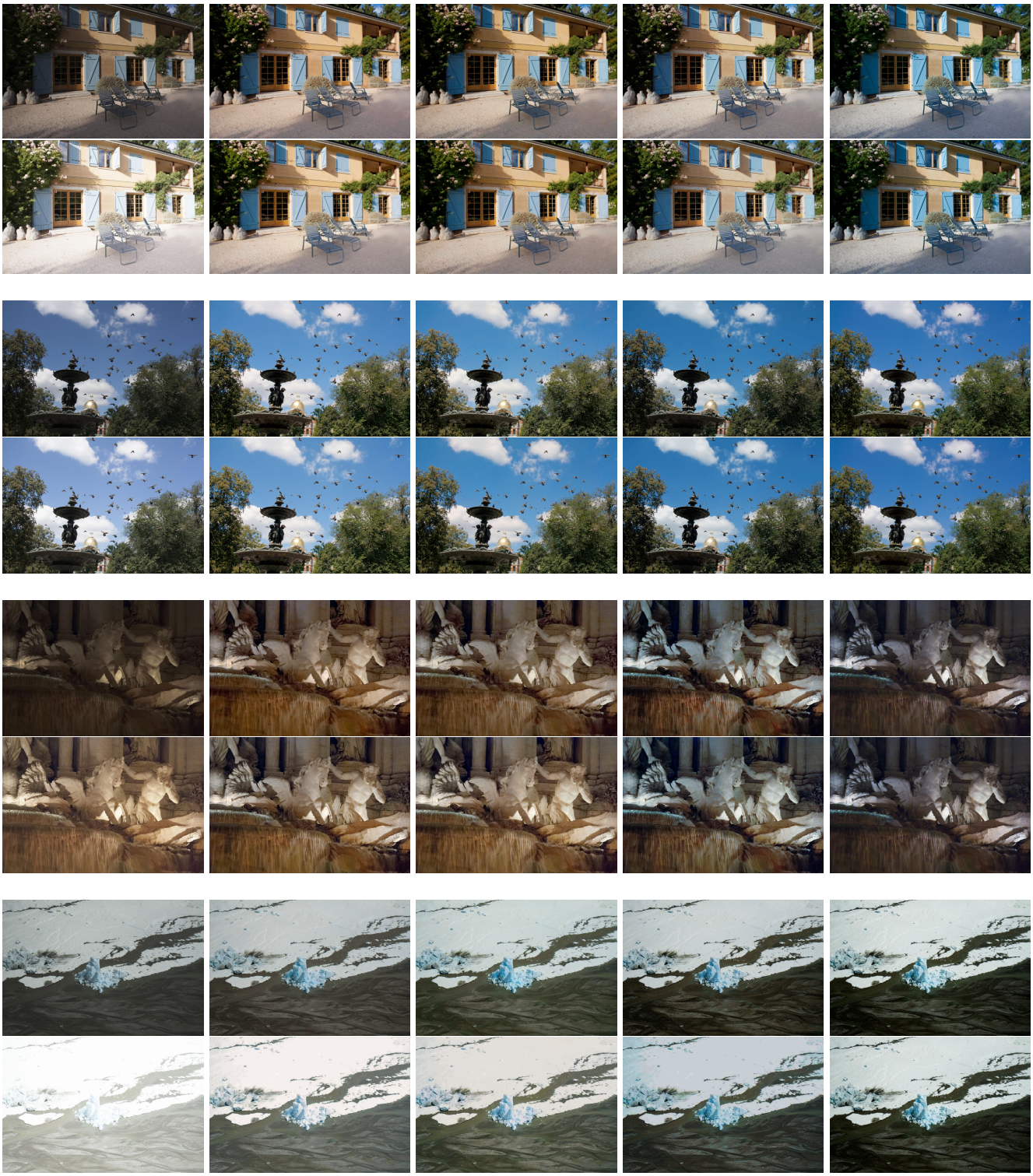

(a) Input image (b) DBRN-ENC [3] (c) FECNet [4] (d) Ours (e) Ground-truth

Figure S-2. Qualitative results on underexposure (odd row) and overexposure (even row) images on the ME dataset.

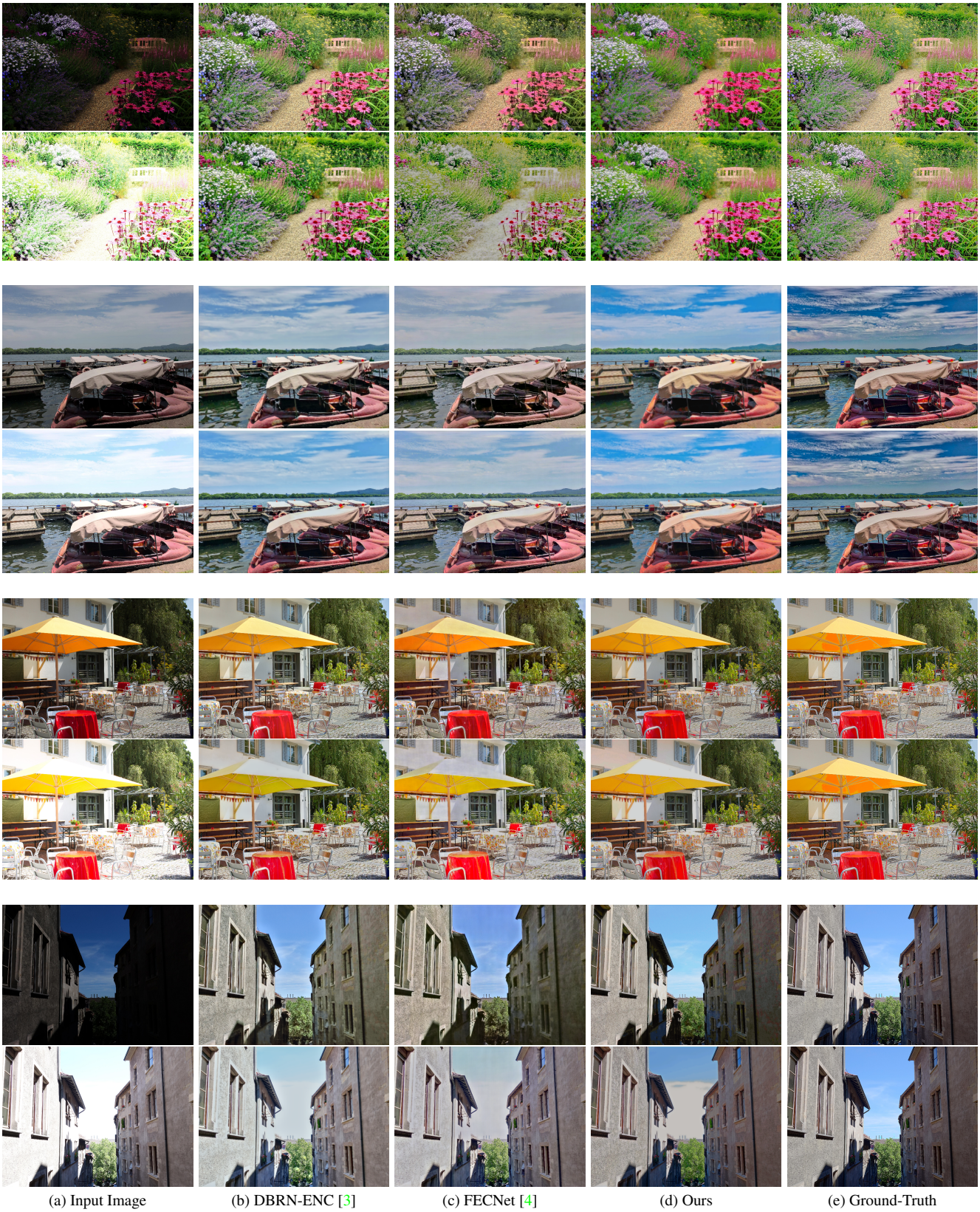

(a) Input Image (b) DBRN-ENC [3] (c) FECNet [4] (d) Ours (e) Ground-Truth

Figure S-3. Qualitative results on underexposure (odd row) and overexposure (even row) images on the SICE dataset.

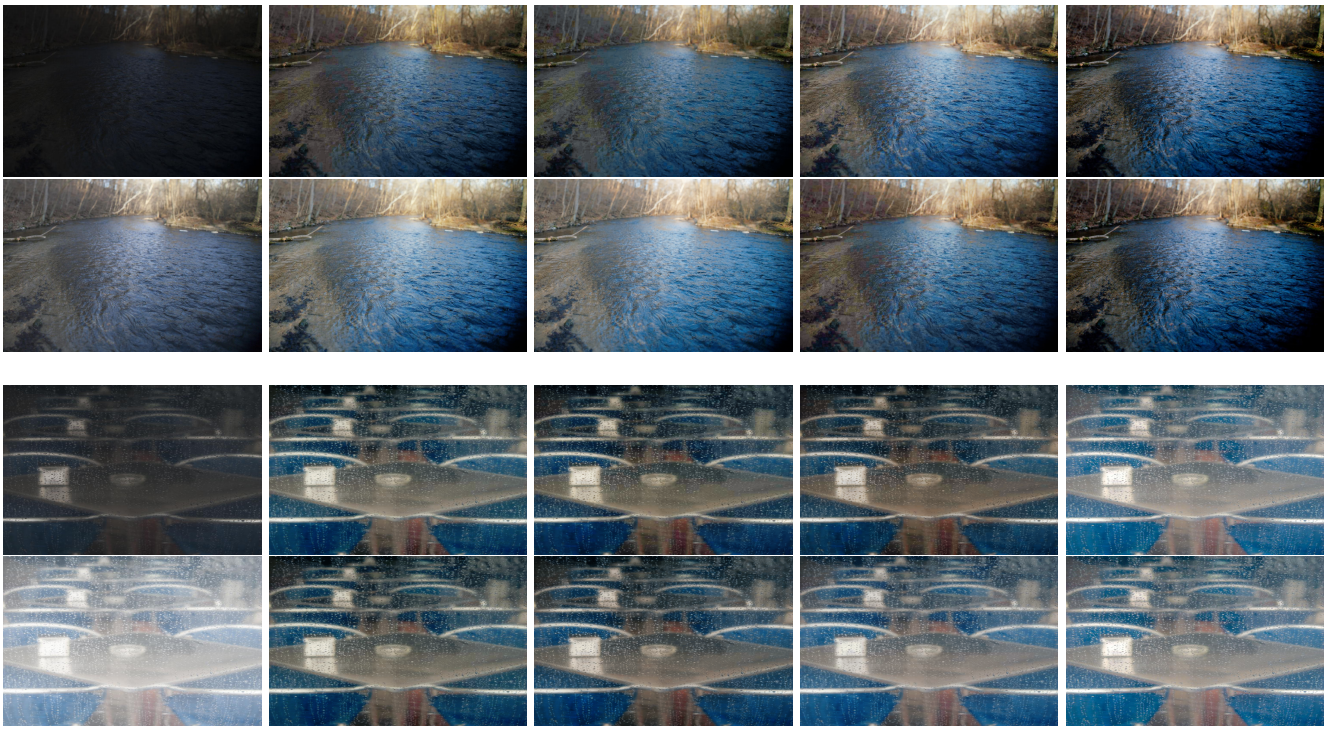

(a) Input image (b) w/o LCM (c) w/o order learning (d) Ours (e) Ground-truth

Figure S-4. Qualitative results on underexposure (odd row) and overexposure (even row) images with different LCM settings on ME.

(a) Input image (b) w/o LCM (c) w/o order learning (d) Ours (e) Ground-truth

Figure S-5. Qualitative results on underexposure (odd row) and overexposure (even row) images with different LCM settings on SICE.